particles

IMPACT FACTOR 1.7

CITESCORE 3.2

Review

Lepton Flavour Universality Tests Using Semileptonic b-Hadron Decays at the LHCb Detector

Bogdan Kutsenko

Special Issue

Selected Papers from the 13th International Conference on New Frontiers in Physics (ICNFP 2024)

Edited by

Prof. Dr. Larissa Bravina, Prof. Dr. Sonia Kabana and Prof. Dr. Armen Sedrakian

MDPI

https://doi.org/10.3390/particles8010005

particles

MDPI

Review

Lepton Flavour Universality Tests Using Semileptonic b-Hadron Decays at the LHCb Detector †

Bogdan Kutsenko on behalf of the LHCb Collaboration

Aix Marseille Univ, CNRS/IN2P3, CPPM, 13009 Marseille, France; bogdan.kutsenko@cern.ch

† This paper is based on the talk at the 13th International Conference on New Frontiers in Physics (ICNFP 2024), Crete, Greece, 26 August–4 September 2024.

Abstract: This review highlights advancements in testing Lepton Flavour Universality (LFU) through semileptonic b-hadron decays at the LHCb detector. Measurements of the LFU $R(D)$ and $R(D^*)$ provide evidence of deviations from Standard Model (SM) predictions, suggesting the presence of possible New Physics (NP). However, the $D^\star$ longitudinal polarisation results are in good agreement with SM expectations, placing constraints on potential NP theories, such as the leptoquarks or charged Higgs models. Further improvements in the measurements' precision are expected with the new data from LHCb Run 3, collected with higher instantaneous luminosity and improved trigger.

Keywords: Lepton Flavour Universality; semileptonic b-hadron decays; LHCb detector

1. Introduction

The semileptonic b-hadron decays, such as $H_b \to H_c \ell \nu$, involve a b-quark hadron H_b, a charm hadron H_c, a charged lepton ℓ, and a neutrino ν. In the Standard Model (SM), these decays proceed via tree-level charged current processes mediated by the W boson. The semileptonic decays of b-hadrons are critical tools for probing the SM and exploring potential New Physics (NP). The SM predicts identical electroweak couplings for all generations of leptons, and this fundamental principle is known as Lepton Flavour Universality (LFU). The measurements of LFU are commonly expressed as ratios of branching fractions, $R(D^{(*)})$, defined as follows:

$$R(D^{(*)}) = \frac{\mathcal{B}(B \to D^{(*)} \ell \nu_\ell)}{\mathcal{B}(B \to D^{(*)} \mu \nu_\mu)}. \quad (1)$$

The processes involving charge conjugates are implicitly included throughout this review. At present, there is a notable discrepancy in the global averages of the LFU $R(D^{(*)})$ ratio, where experimental values diverge from SM predictions by more than three standard deviations (3σ) in the case of τ/μ universality [1]. This inconsistency raised significant interest in whether NP could explain the observed tension. Deviations from LFU could indicate contributions from processes such as interactions mediated by leptoquarks [2] or charged Higgs bosons [3].

Furthermore, angular analysis can provide additional evidence and discriminate between the models. Even when the branching fraction ratios are perfectly compatible with the SM predictions, NP currents can still impact angular distributions.

This report highlights the following recent LHCb contributions to LFU tests: the measurement of $R(D^{(*)+})$ in the muonic mode of τ decay: $\tau^- \to \mu^- \bar{\nu}_\mu \nu_\tau$ [4], $R(D^{(*)})$ and in the hadronic mode of τ decay: $\tau^- \to \pi^- \pi^+ \pi^- (\pi^0) \nu_\tau$ [5]; and the analysis of

Academic Editors: Larissa Bravina, Sonia Kabana and Armen Sedrakian

Received: 26 December 2024
Revised: 8 January 2025
Accepted: 10 January 2025
Published: 14 January 2025

Citation: Kutsenko, B., on behalf of the LHCb Collaboration. Lepton Flavour Universality Tests Using Semileptonic b-Hadron Decays at the LHCb Detector. *Particles* **2025**, *8*, 5. https://doi.org/10.3390/particles8010005

the longitudinal polarisation of D^{*+} in the decay $B^0 \to D^{*+}\tau^-\nu_\tau$ [6]. These studies use efficient triggers, and they demonstrate the excellent tracking and vertexing performance and powerful particle identification of the LHCb detector [7].

2. $\mathcal{R}(D^{*+})$ and $\mathcal{R}(D^+)$ Measurements in the Muonic Mode

This study focuses on the first simultaneous measurement of the lepton universality ratios $R(D^+)$ and $R(D^{*+})$ using muonic τ lepton decays in $B^0 \to D^+\tau^-\nu_\tau$ and $B^0 \to D^{*+}\tau^-\nu_\tau$ decays. Data were collected by the LHCb experiment in 2015–2016, corresponding to an integrated luminosity of 2.0 fb^{-1} from pp collisions at centre-of-mass collision energy $\sqrt{s} = 13$ TeV. To extract the branching fractions, a three-dimensional binned likelihood fit is used in the variables q^2 (four-momentum transfer squared), E_μ^* (muon energy in the B-meson frame), and m^2_{miss} (missing mass squared). This approach maximises signal-to-background separation by leveraging kinematic differences, with templates derived from simulation and validated using control regions, ensuring that corrections derived from the control regions are consistently propagated to the signal region.

Several methodological advancements were employed to address the experimental challenges posed by multiple neutrinos in the final state and the need for partial reconstruction. To validate the neutrino reconstruction procedure and to extract efficiencies and the signal yield, a high-statistics MC sample is required. Traditional full simulation methods are computationally expensive. This study employs a tracker-only simulation technique, which does not include a detailed simulation of photon propagation in the RICH detectors and calorimeter shower development. This approach reduces simulation time by a factor of eight and event size by 40%, while maintaining accuracy. Validation against the full simulation was conducted.

Background isolation techniques are applied, including a boosted decision tree (BDT) for neutral isolation to suppress backgrounds from $B^0 \to D^{*+}\tau^-\nu_\tau$ decays involving neutral pions and a second BDT for track isolation that prioritises additional charged tracks consistent with D^+ production, suppressing combinatorial backgrounds.

The dataset is split into four categories based on the response of the track isolation tool. The first category, known as the *signal region*, is defined by the absence of any tracks near the signal candidate. Two additional categories, the *one-pion* and *two-pion regions*, include events with exactly one or two additional charged pions, respectively. These regions are used to refine and validate the modelling of background contributions from D^{**} states ($D^*(2007)^+$ and $D^*(2010)^0$), which represent excited charm mesons that are heavier than the first excited states in the signal decay. The fourth category, *one-kaon region*, contains events with an additional charged kaon and is employed to control background contributions from $B \to D^+(X_c \to \mu^- X)(X')$ decays. Here, X_c represents a charm hadron that often produces charged kaons, while X denotes other unreconstructed particles. All four regions are fitted simultaneously.

Same-sign $D^+\mu^+$ pairs are used to model the combinatorial background, efficiently suppressing random track combinations. Simulation is corrected for discrepancies with data in geometric (track reconstruction) and kinematic (momentum and energy distributions) properties. A weight-based calibration corrects kinematic variables like m^2_{miss}, q^2, and the Dalitz plot in $D^+ \to K^-\pi^+\pi^+$ decays. A multivariate selection combines kinematic variables, particle identification (PID) criteria, and the impact parameter constraints for the high-purity selection of D^+ candidates. Neural networks are employed to reject fake tracks. Signal and normalisation yields are derived from multi-dimensional fits in the signal and control regions, as shown in Figure 1.

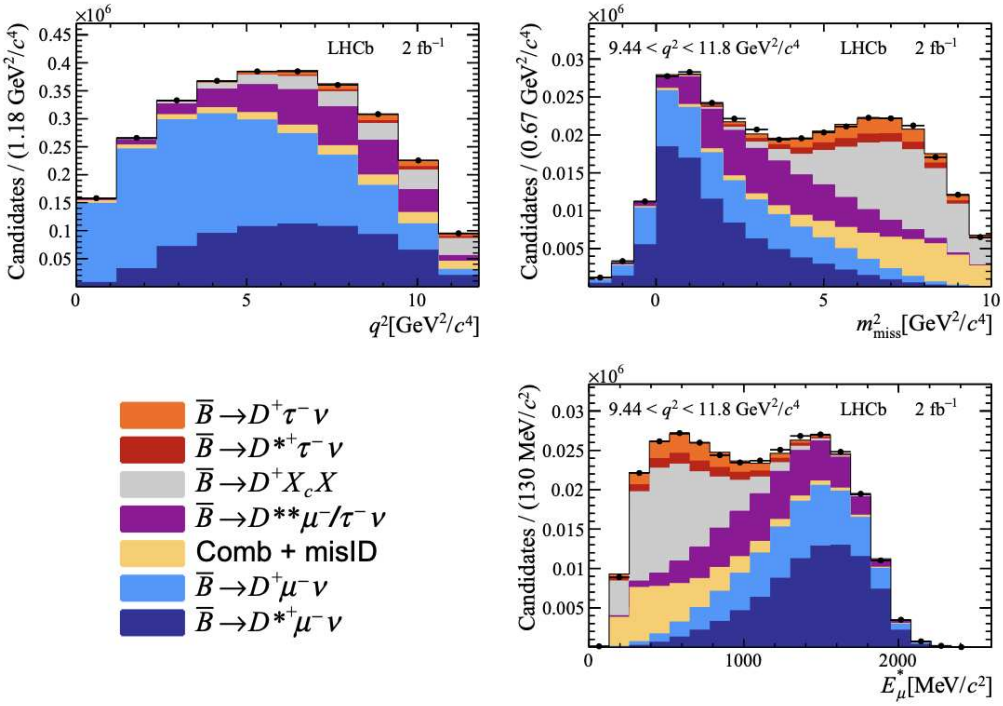

Figure 1. Distributions of the three kinematic variables in the signal isolation region with the fit result superimposed. The q^2 distribution is displayed across the entire fit range, while m^2_{miss} and E^*_μ are shown only for the range $9.44 < q^2 < 11.8\,\text{GeV}^2/c^4$.

The branching fraction ratios are determined as follows:

$$R(D^+) = 0.249 \pm 0.043\,(\text{stat}) \pm 0.047\,(\text{syst}), \tag{2}$$

$$R(D^{*+}) = 0.402 \pm 0.081\,(\text{stat}) \pm 0.085\,(\text{syst}), \tag{3}$$

with a Pearson correlation coefficient of -0.39. Systematic variations in the form factors were used to test alternative decay hypotheses. Form-factor modelling, misidentification rates, and simulation statistics dominate systematic uncertainties. These measurements are consistent with Standard Model predictions within the following uncertainties [1]: $R_{D^*} = 0.254(5)$ and $R_{D^+} = 0.296(4)$.

3. $\mathcal{R}(D^*)$ Measured in Hadronic Mode

The LHCb hadronic $R(D^*)$ analysis was initially conducted using proton–proton (pp) collision data, collected at centre-of-mass energies of $\sqrt{s} = 7$ and 8 TeV during 2011 and 2012 [8], corresponding to an integrated luminosity of $3\,\text{fb}^{-1}$. The similar measurement of hadronic $R(D^*)$ was performed based on pp collision data collected at 13 TeV in 2015 and 2016, with an integrated luminosity of $2\,\text{fb}^{-1}$. Despite the lower integrated luminosity, the approximately two-fold increase in the $b\bar{b}$ production cross section at the higher centre-of-mass energy and enhancements in the LHCb trigger result in about 40% more signal candidates compared to the previous analysis.

The τ^+ lepton is reconstructed in the hadronic final state $3\pi(\pi^0)\bar{\nu}_\tau$, where $3\pi \equiv \pi^+\pi^-\pi^+$ and the D^{*-} candidate are reconstructed via the decay $D^{*-} \to \pi^-\bar{D}^0(\to K^+\pi^-)$. The $B^0 \to D^{*-}3\pi$ decay is used as the normalisation mode, as it shares the same visible final state as the signal mode. This choice minimises systematic uncertainties related to detector and reconstruction effects in the ratio of their branching fractions as follows:

$$K(D^{*-}) = \frac{\mathcal{B}(B^0 \to D^{*-}\tau^+\nu_\tau)}{\mathcal{B}(B^0 \to D^{*-}3\pi)} = \frac{N_{\text{sig}}}{N_{\text{norm}}} \cdot \frac{\varepsilon_{\text{norm}}}{\varepsilon_{\text{sig}}} \cdot \frac{1}{\mathcal{B}(\tau^+ \to 3\pi\bar{\nu}_\tau) + \mathcal{B}(\tau^+ \to 3\pi\pi^0\bar{\nu}_\tau)}. \quad (4)$$

Here, N_{sig} and N_{norm} represent the yields for the signal and normalisation modes, respectively, as extracted from data. The efficiencies ε_{sig} and $\varepsilon_{\text{norm}}$ for the signal and normalisation modes are determined from MC.

The signal efficiency, ε_{sig}, is determined from the simulation as the weighted average of the $\tau^+ \to 3\pi\bar{\nu}_\tau$ and $\tau^+ \to 3\pi\pi^0\bar{\nu}_\tau$ decay channels, with weights proportional to their respective branching fractions. Subsequently, using the known branching fractions $\mathcal{B}(B^0 \to D^{*-}3\pi)$ and $\mathcal{B}(B^0 \to D^{*-}\mu^+\nu_\mu)$ [9], the value of $R(D^{*-})$ is calculated as follows:

$$R(D^{*-}) = K(D^{*-}) \frac{\mathcal{B}(B^0 \to D^{*-}3\pi)}{\mathcal{B}(B^0 \to D^{*-}\mu^+\nu_\mu)}, \quad (5)$$

The reconstruction of decay kinematics follows the methodology outlined in Ref. [8]. Signal candidates are formed by combining a D^{*-} meson decaying as $D^{*-} \to \pi^-\overline{D}^0(\to K^+\pi^-)$ with a 3π system detached from the B^0 decay vertex due to the τ^+ lepton's finite lifetime. Key parameters for background suppression include vertex separation and momentum selection, with Boosted Decision Tree (BDT) classifiers further enhancing background rejection.

The following three data categories were used: *signal*, *normalisation*, and *control*. Control samples enrich D_s^+ decays for background studies and are used to derive corrections for simulated samples. These corrections are crucial for obtaining the accurate probability density functions (PDFs) used in the fit to determine the signal yield.

The $B^0 \to D^{*-}\tau^+\nu_\tau$ yield is extracted via a 3D template fit to q^2, τ decay time (t_τ), and anti-D_s^+ BDT output, as shown in Figure 2. The fit accounts for signal and background components, including double-charm decays, combinatorial backgrounds, and misidentified tracks. Key background parameters are constrained using control sample results. The signal yield is $N_{\text{sig}} = 2469 \pm 154$ events (statistical uncertainty only), with excellent fit quality ($\chi^2/\text{n.d.f.} = 1.0$).

Using the yields and efficiencies for $B^0 \to D^{*-}\tau^+\nu_\tau$ and $B^0 \to D^{*-}3\pi$, the ratio $K(D^{*-})$ is measured as follows:

$$K(D^{*-}) = 1.70 \pm 0.10\,(\text{stat})\,^{+0.11}_{-0.10}\,(\text{syst}). \quad (6)$$

The result is consistent with the previous BaBar, Belle, and LHCb measurements [8]. The updated analysis procedure improves signal efficiency and reduces the relative systematic uncertainty from 9% to 6%. Using the latest branching fraction measurements [9],

$$\mathcal{B}(B^0 \to D^{*-}3\pi) = (7.21 \pm 0.29) \times 10^{-3} \quad (7)$$

and

$$\mathcal{B}(B^0 \to D^{*-}\mu^+\nu_\mu) = (4.97 \pm 0.12)\%, \quad (8)$$

the branching fraction

$$\mathcal{B}(B^0 \to D^{*-}\tau^+\nu_\tau) = (1.23 \pm 0.07\,(\text{stat})\,^{+0.08}_{-0.07}\,(\text{syst}) \pm 0.05\,(\text{ext})) \times 10^{-2}, \quad (9)$$

and the ratio of branching fractions

$$R(D^{*-}) = 0.247 \pm 0.015\,(\text{stat}) \pm 0.015\,(\text{syst}) \pm 0.012\,(\text{ext}), \quad (10)$$

are obtained. The third uncertainty reflects the external branching fraction uncertainties. These results agree with the current world average and the Standard Model expectation of $R(D^{*-}) = 0.254 \pm 0.005$ [1].

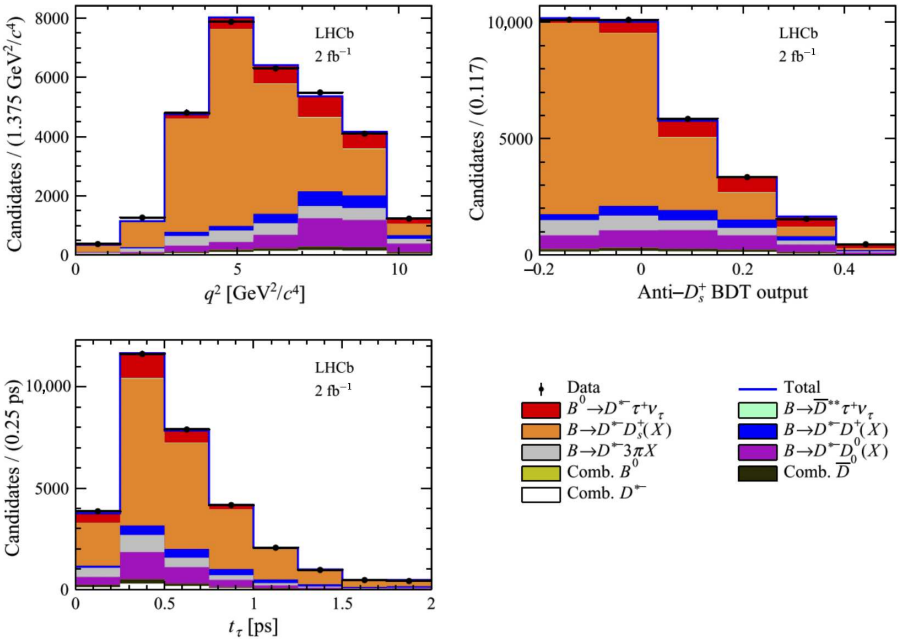

Figure 2. Distributions of the fit variables for the $B^0 \to D^-\tau^+\nu_\tau$ data sample.

4. D^* Longitudinal Polarisation

The D^* longitudinal polarisation fraction, $F_{D^*}^L$, provides sensitivity to NP operators. New scalar operators could lead to an increase in the value of F_{D^*}, while new tensor operators may suppress it. The fraction is defined as follows:

$$F_{D^*}^L(q^2) = \frac{a_{\theta_D}(q^2) + c_{\theta_D}(q^2)}{3a_{\theta_D}(q^2) + c_{\theta_D}(q^2)}, \tag{11}$$

where θ_D is the angle between the D^0 meson direction and the opposite direction of the B^0 meson in the D^* rest frame. The quantity q^2 represents the squared invariant mass of the $\tau\nu_\tau$ system, computed from the squared difference between the momenta of the B and D^* mesons. The coefficients $a_{\theta_D}(q^2)$ and $c_{\theta_D}(q^2)$ are linear combinations of twelve angular coefficients, which include both the hadronic effects and the fundamental couplings [6]. The angular coefficients characterise the decay width.

Using 5 fb^{-1} of data, LHCb measured $F_{D^*}^L$ in two q^2 regions as follows:

$$F_{D^*}^L(q^2 < 7\,\text{GeV}^2) = 0.51 \pm 0.07\,(\text{stat.}) \pm 0.03\,(\text{syst.}), \tag{12}$$

$$F_{D^*}^L(q^2 > 7\,\text{GeV}^2) = 0.35 \pm 0.08\,(\text{stat.}) \pm 0.02\,(\text{syst.}). \tag{13}$$

The parameters $a_{\theta_D}(q^2)$ and $c_{\theta_D}(q^2)$ are obtained by dividing the simulated signal template into the following two components: one represents the completely unpolarised case with non-zero $a_{\theta_D}(q^2)$ and the other one represents the completely polarised case with non-zero $c_{\theta_D}(q^2)$. The number of polarised and unpolarised signal events is determined through an extended maximum-likelihood fit to the four-dimensional distribution of $\cos\theta_D$, q^2, t_τ, and the anti-D_s^+ BDT output shown in Figure 3. The free parameters include the following:

- $N_{\text{unpol}}^{\text{low } q^2}$ and $N_{\text{unpol}}^{\text{high } q^2}$: unpolarised signal events in the low- and high-q^2 regions.

- $f_{pol}^{low\ q^2}$ and $f_{pol}^{high\ q^2}$: fractions of polarised signal events in low- and high-q^2 regions.
- Additional parameters account for background and specific decay modes.

Some parameters are fixed or constrained to improve fit stability, such as the branching ratios and fractions of the background contributions. The fit achieves a $\chi^2/\text{n.d.f.} = 806/736$, with results summarised in Table 1.

The extracted fractions of polarised events are 0.361 ± 0.074 (stat) and 0.013 ± 0.081 (stat) for the low- and high-q^2 regions, respectively. The derived values of $a_{\theta_D}(q^2)$, $c_{\theta_D}(q^2)$, and $F_{D^*}^L$ across the q^2 range are provided in Table 2.

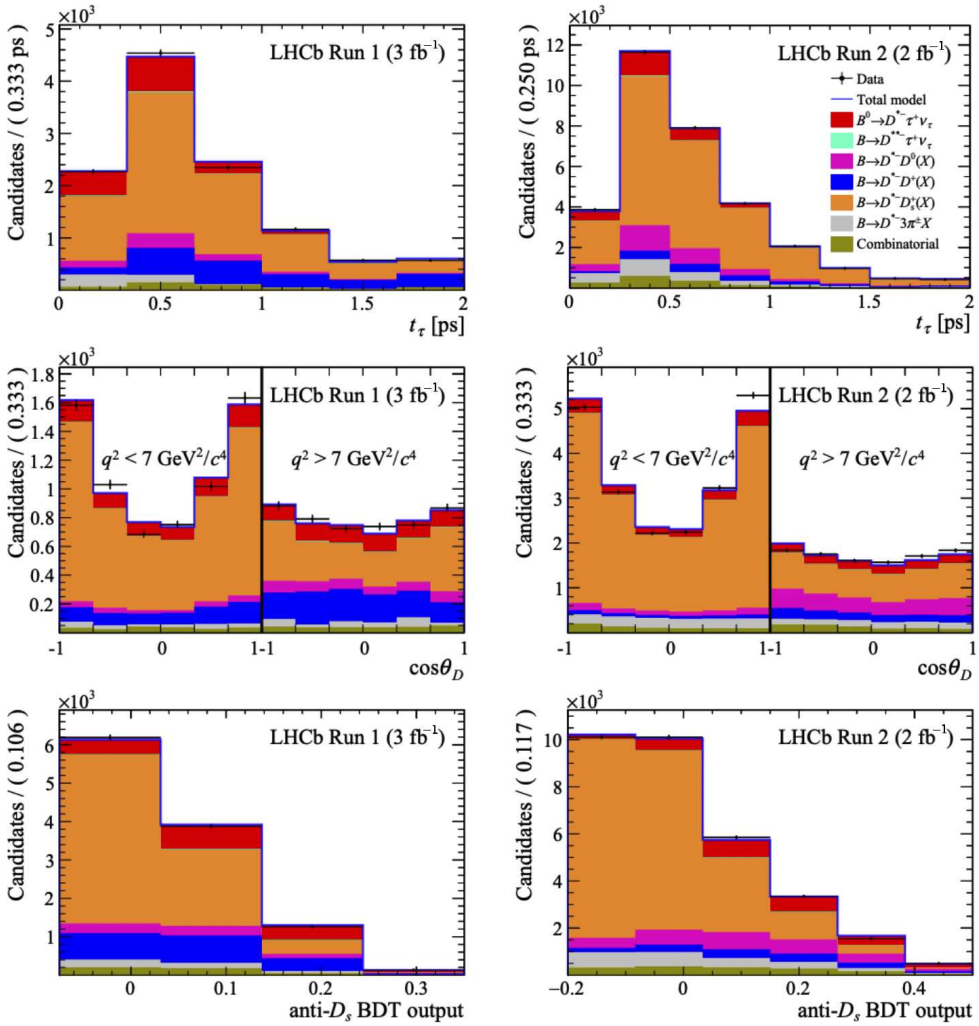

Figure 3. Distributions of the fit variables for the (**left**) Run 1 and (**right**) Run 2 datasets, with the corresponding fit results overlaid.

Table 1. Fit results for the Run 1 and Run 2 datasets.

Parameter	Run 1	Run 2
$N_{unpol}^{low\ q^2}$	360 ± 55	758 ± 62
$N_{unpol}^{high\ q^2}$	532 ± 70	827 ± 109
$f_{pol}^{low\ q^2}$	0.36 ± 0.07	—
$f_{pol}^{high\ q^2}$	0.01 ± 0.08	—

Table 2. Values of $a_{\theta_D}(q^2)$, $c_{\theta_D}(q^2)$, and $F^L_{D^*}$.

Parameter	$q^2 < 7$ GeV$^2/c^4$	$q^2 > 7$ GeV$^2/c^4$	Whole q^2 Range
$a_{\theta_D}(q^2)$	0.12 ± 0.02	0.15 ± 0.03	0.14 ± 0.03
$c_{\theta_D}(q^2)$	0.13 ± 0.05	0.01 ± 0.02	0.07 ± 0.06
$F^L_{D^*}$	0.51 ± 0.07	0.35 ± 0.08	0.43 ± 0.06

These values are consistent with SM predictions and improve constraints on scalar and tensor NP operators.

5. Conclusions

LHCb's recent advances mark significant progress in testing LFU as follows:

- Improved precision in $R(D^{(*)})$ measurements, as shown in Figure 4.
- The first LHCb observation of D^* longitudinal polarisation.
- Improved methodology, including fast simulation techniques and refined background modelling.

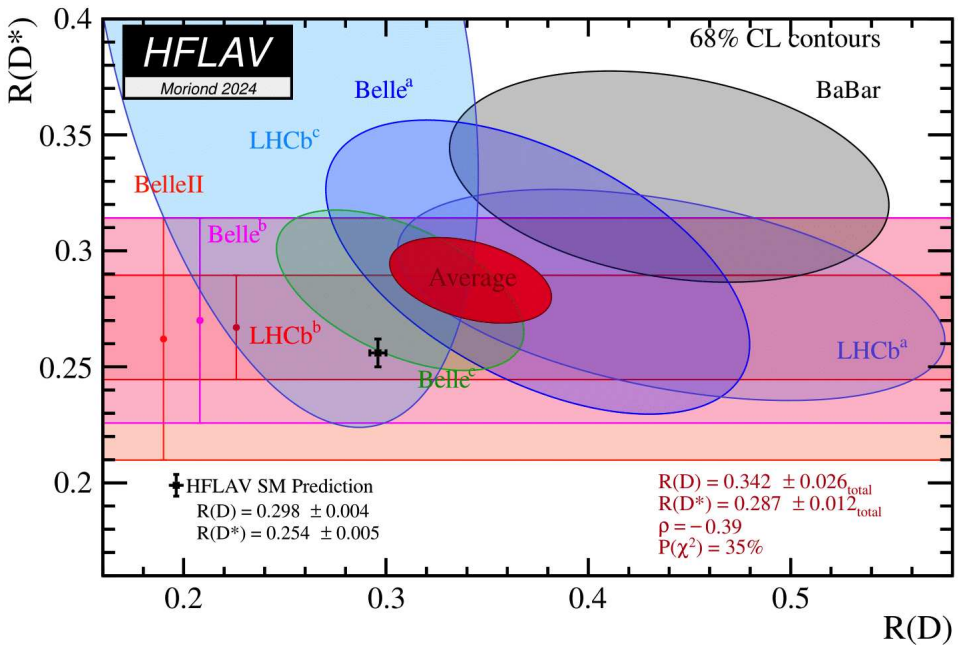

Figure 4. Illustrative overview of measured values of the ratios $R(D)$ and $R(D^*)$ from the Belle [10–12], Belle II [13], BaBar [3,14], and LHCb [5,15–17] experiments, updated to summer 2024 [1]. The contours represent a 68% confidence level, corresponding to 1 σ in a normal distribution. The black and blue markers indicate the Standard Model (SM) predictions, while the combined experimental results from LHCb, Belle, and BaBar are shown as a red ellipse. The red dashed lines mark the 3 σ confidence region.

The $R(D^{(*)})$ measurements, which deviate from SM predictions by 3.3σ, align well with earlier results from Belle and BaBar. The ongoing discrepancy with Standard Model predictions supports the possibility of New Physics contributions, such as leptoquarks or new gauge bosons with enhanced couplings to third-generation fermions. At the same time, the agreement of $F^L_{D^*}$ with SM expectations imposes stringent constraints, ruling out certain scalar and tensor operators in NP models.

Looking ahead, the upcoming Run 3 of the LHC can further enhance these measurements by increasing the instantaneous luminosity by a factor of five and improving the

trigger efficiency for most modes by a factor of two [18]. The annual yields in most channels is in an order of magnitude larger than that of previous LHCb experiment, offering an opportunity to resolve the current discrepancies and deepen our understanding of the fundamental interactions.

Funding: This research received no external funding.

Data Availability Statement: No new data were created.

Conflicts of Interest: The authors declare no conflicts of interest.

References

1. Banerjee, S.; Ben-Haim, E.; Bernlochner, F.; Bertholet, E.; Bona, M.; Bozek, A.; Bozzi, C.; Brodzicka, J.; Chobanova, V.; Chrzaszcz, M.; et al. Averages of b-hadron, c-hadron, and τ-lepton properties as of 2023. *arXiv* **2023**, arXiv:2411.18639.
2. Davidson, S.; Bailey, D.; Campbell, B.A. Model independent constraints on leptoquarks from rare processes. *Z. FÜr Phys. Part. Fields* **1994**, *61*, 613. [CrossRef]
3. BaBar Collaboration; Lees, J.P. Measurement of an excess of decays and implications for charged Higgs bosons. *Phys. Rev. D* **2013**, *88*, 072012. [CrossRef]
4. LHCb Collaboration. Measurement of the branching fraction ratios $r(D^+)$ and $r(D^{*+})$ using muonic τ decays. *arXiv* **2024**, arXiv:2406.03387.
5. LHCb Collaboration; Aaij, R.; Abdelmotteleb, A.S.W.; Beteta, C.A.; Abudinén, F.; Achard, C.; Ackernley, T.; Adeva, B.; Adinolfi, M.; Adlarson, P.; et al. Test of lepton flavor universality using $B^0 \to D^{*-}\tau^+\nu_\tau$ decays with hadronic τ channels. *Phys. Rev. D* **2024**, *108*, 012018. [CrossRef]
6. Aaij, R.; Abdelmotteleb, A.S.W.; Abellan Beteta, C.; Abudinén, F.; Ackernley, T.; Adeva, B.; Adinolfi, M.; Adlarson, P.; Afsharnia, H.; Agapopoulou, C.; et al. Measurement of the D^* longitudinal polarization in $B^0 \to D^{*-}\tau^+\nu_\tau$ decays. *arXiv* **2023**, arXiv:2311.05224. [CrossRef]
7. LHCb Collaboration. LHCb detector performance. *Int. J. Mod. Phys. A* **2023**, *30*, 1530022. [CrossRef]
8. Aaij, R.; Beteta, C.A.; Adametz, A.; Adeva, B.; Adinolfi, M.; Adrover, C.; Affolder, A.; Ajaltouni, Z.; Albrecht, J.; Alessio, F.; et al. Measurement of the Ratio of Branching Fractions $\mathcal{B}(\overline{B}^0 \to D^{*+}\tau^-\overline{\nu}_\tau)/\mathcal{B}(\overline{B}^0 \to D^{*+}\mu^-\overline{\nu}_\mu)$. *Phys. Rev. Lett.* **2015**, *115*, 111803. [CrossRef] [PubMed]
9. Navas, S.; Amsler, C.; Gutsche, T.; Hanhart, C.; Hernández-Rey, J.J.; Lourenço, C.; Masoni, A.; Mikhasenko, M.; Mitchell, R.E.; Patrignani, C.; et al. Review of Particle Physics. *Phys. Rev. D* **2024**, *110*, 030001. [CrossRef]
10. Belle Collaboration; Huschle, M.; Kuhr, T.; Heck, M.; Goldenzweig, P.; Abdesselam, A.; Adachi, I.; Adamczyk, K.; Aihara, H.; Said, S.A.; et al. Measurement of the branching ratio of $B \to D^{(*)}\tau^-\nu_\tau$ relative to $B \to D^{(*)}\ell^-\nu_\ell$ decays with hadronic tagging at Belle. *Phys. Rev. D* **2015**, *92*, 072014. [CrossRef]
11. Belle Collaboration; Hirose, S.; Iijima, T.; Adachi, I.; Adamczyk, K.; Aihara, H.; Said, S.A.; Asner, D.M.; Atmacan, H.; Aulchenko, V.; et al. Measurement of the τ lepton polarization and $R(D^*)$ in the decay $B \to D^*\tau^-\nu_\tau$. *Phys. Rev. Lett.* **2017**, *118*, 211801. [CrossRef] [PubMed]
12. Belle Collaboration; Caria, G.; Urquijo, P.; Adachi, I.; Aihara, H.; Said, S.A.; Asner, D.M.; Atmacan, H.; Aushev, T.; Babu, V.; et al. Measurement of $R(D)$ and $R(D^*)$ with a semileptonic tagging method. *Phys. Rev. Lett.* **2020**, *124*, 161803. [CrossRef] [PubMed]
13. Belle-II Collaboration; Adachi, I.; Adamczyk, K.; Aggarwal, L.; Ahmed, H.; Aihara, H.; Akopov, N.; Aloisio, A.; Ky, N.A.; Asner, D.M.; et al. A test of lepton flavor universality with a measurement of $R(D^*)$ using hadronic B tagging at the Belle II experiment. Available online: https://arxiv.org/abs/2401.02840 (accessed on 12 January 2025).
14. BABAR Collaboration; Lees, J.P.; Poireau, V.; Tisserand, V.; Grauges, E.; Palano, A.; Eigen, G.; Brown, D.N.; Kolomensky, Y.G.; Fritsch, M.; et al. Evidence for an excess of $B \to D^{(*)}\tau^-\nu_\tau$ decays. *Phys. Rev. Lett.* **2012**, *109*, 101802. [CrossRef] [PubMed]
15. LHCb Collaboration; Aaij, R.; Abdelmotteleb, A.S.W.; Beteta, C.A.; Abudinén, F.; Achard, C.; Ackernley, T.; Adeva, B.; Adinolfi, M.; Adlarson, P.; et al. Measurement of the ratios of branching fractions $R(D^*)$ and $R(D^0)$. *Phys. Rev. Lett.* **2023**, *131*, 111802. [CrossRef] [PubMed]
16. LHCb Collaboration; Aaij, R.; Adeva, B.; Adinolfi, M.; Ajaltouni, Z.; Akar, S.; Albrecht, J.; Alessio, F.; Alexander, M.; Albero, A.A.; et al. Measurement of the ratio of the $B^0 \to D^{*-}\tau^+\nu_\tau$ and $B^0 \to D^{*-}\mu^+\nu_\mu$ branching fractions using three-prong τ-lepton decays. *Phys. Rev. Lett.* **2018**, *120*, 171802. [CrossRef] [PubMed]

17. LHCb Collaboration; Aaij, R.; Adeva, B.; Adinolfi, M.; Ajaltouni, Z.; Akar, S.; Albrecht, J.; Alessio, F.; Alexander, M.; Albero, A.A.; et al. Test of Lepton Flavor Universality by the measurement of the $B^0 \to D^{*-}\tau^+\nu_\tau$ branching fraction using three-prong τ decays. *Phys. Rev. D* **2018**, *97*, 072013. [CrossRef]
18. LHCb Collaboration; Aaij, R.; Abdelmotteleb, A.S.W.; Beteta, C.A.; Abudinén, F.; Achard, C.; Ackernley, T.; Adeva, B.; Adinolfi, M.; Adlarson, P.; et al. The LHCb Upgrade I. *J. Instrum.* **2024**, *19*, P05065. [CrossRef]